



CHORUS

This is the accepted manuscript made available via CHORUS. The article has been published as:

Efimov effect for heteronuclear three-body systems at positive scattering length and finite temperature

Samuel B. Emmons, Daekyoung Kang, Bijaya Acharya, and Lucas Platter

Phys. Rev. A **96**, 032706 — Published 8 September 2017

DOI: [10.1103/PhysRevA.96.032706](https://doi.org/10.1103/PhysRevA.96.032706)

The Efimov effect for heteronuclear three-body systems at positive scattering length and finite temperature

Samuel B. Emmons,^{1,*} Daekyoung Kang,^{2,†} Bijaya Acharya,^{1,‡} and Lucas Platter^{1,3,§}

¹*Department of Physics and Astronomy, University of Tennessee, Knoxville, TN 37996, USA*

²*Theoretical Division, MS B283, Los Alamos National Laboratory, Los Alamos, NM 87545, USA*

³*Physics Division, Oak Ridge National Laboratory, Oak Ridge, TN 37831, USA*

(Dated: August 10, 2017)

We study the recombination process of three atoms scattering into an atom and diatomic molecule in heteronuclear mixtures of ultracold atomic gases with large and positive interspecies scattering length at finite temperature. We calculate the temperature dependence of the three-body recombination rates by extracting universal scaling functions that parametrize the energy dependence of the scattering matrix. We compare our results to experimental data for the ^{40}K - ^{87}Rb mixture and make a prediction for ^6Li - ^{87}Rb . We find that contributions from higher partial wave channels significantly impact the total rate and, in systems with particularly large mass imbalance, can even obliterate the recombination minima associated with the Efimov effect.

*Electronic address: semmons@vols.utk.edu

†Electronic address: kang1@lanl.gov

‡Electronic address: bacharya@utk.edu

§Electronic address: lplatter@utk.edu

I. INTRODUCTION

At sufficiently low energies, the properties of an ultracold gas of atoms are determined by the S-wave scattering length of the atoms. The scattering length, a , is usually of the size of the range of the interaction ℓ . However, there exist systems in nature and in the laboratory, such as nucleons, halo nuclei or atoms in an external magnetic field tuned near a Feshbach resonance, in which $|a| \gg \ell$ [1]. In this case low-energy two-body observables can be expressed in terms of the a and the associated momentum scale $k \sim 1/a$ up to corrections proportional to $k\ell$ and ℓ/a . Three-body systems of identical bosons with large a exhibit a discrete scaling symmetry characterized by log-periodic dependence of observables on an additional parameter κ_* . This is commonly referred to as the Efimov effect, after Vitaly Efimov [2]. Perhaps the most striking manifestation of this effect is the emergence of an infinite sequence of bound states in the unitary limit where $a \rightarrow \pm\infty$, with energies¹

$$E^{(n)} = -\lambda^{2(n_*-n)} \frac{\kappa_*^2}{m}; \quad n = n_*, n_* \pm 1, n_* \pm 2, \dots \quad (1)$$

Here m can be any quantity with the dimension of mass and κ_* is the binding momentum of the three-body state with $n = n_*$. The scaling factor λ depends on the mass ratio of the particles as well as on whether they are identical or distinguishable. For identical particles, it is $\lambda_B \approx 22.694$ [3]. Numerous experiments with ultracold atomic gases consisting of identical bosons have confirmed the existence of the Efimov effect by measuring rates of loss of trapped atoms due to various three-body recombination processes [4–7]. The effect was also confirmed in three distinguishable states of ^6Li atoms [8–15]. Overall, these experiments have found excellent agreement with theoretical calculations on many of the important qualitative and quantitative details of Efimov physics [16].

There has been a recent trend [17–19] towards performing experiments with heteronuclear systems consisting of two species of atoms with a large interspecies scattering length, where λ can be driven away from λ_B [3]. Using light-heavy mixtures thus engenders a more precise and detailed understanding of Efimov physics by making a larger number of Efimov states experimentally accessible. Theoretical studies of Efimov physics in such systems have been performed with zero-range interactions for zero [20] and large [21] intraspecies scattering length. Finite-range potential models were used in Refs. [22, 23]. By extending the effective-field-theory analysis of Ref. [20], model-independent inclusion of the leading corrections due to finite interaction ranges and intraspecies scattering length was performed in Ref. [24]. All of the above-mentioned theoretical studies have focused on the idealized scenario in which the temperature of the heteronuclear mixture is exactly zero. However, in real experimental situations the temperature of the gas, though small, typically ranges from nK to μK . This introduces an additional length scale—the thermal de Broglie wavelengths in the gas—that leads to additional modifications of the discrete scaling laws. The finite temperature effects can be taken into account by generalizing the S -matrix formalism developed to calculate loss-rates for three-boson systems in Refs. [3, 25] to the heteronuclear system. In Ref. [26], this was done for systems that do not support weakly bound two-body subsystems, *i.e.* when the interspecies scattering length is negative. The purpose of the present work is to study the temperature dependence of three-body recombination in two-species mixtures of ultracold atomic gases when the interspecies scattering length is large and positive, leading to the existence of a shallow diatomic molecule, while the scattering length between atoms of the same species remains negligible. We perform a detailed analysis of the contribution of different partial waves to the thermal-averaged recombination rate. We present our results for two systems of experimental interest, ^{40}K - ^{87}Rb and ^6Li - ^{87}Rb .

The rest of this paper is organized as follows. In Sec. II, we briefly review the calculation of the phase shifts for the scattering of an atom by a diatomic molecule using the Skorniakov–Ter-Martirosian (STM) integral equation [27], which was originally applied to the scattering of low-energy neutrons by deuterons and has been widely used in atomic physics to study the low-energy scattering of atoms by dimers [28, 29]. Section III then details how the formalism of Refs. [3, 25] can be extended to the heteronuclear case in order to relate the scattering phase shifts to the universal scaling functions that parameterize the three-body recombination rates. Next, we calculate the temperature-dependent three-body recombination rate constant as a function of the scattering length and compare to experimental data in Sec. IV. We present our concluding remarks in Sec. V.

II. STM EQUATION, SCATTERING AMPLITUDE, AND PHASE SHIFTS

We consider three-body heteronuclear systems ($A_1A_2A_2$) wherein the interspecies S-wave scattering length a is large and positive, but the scattering length between any identical atoms is negligible. A diatomic molecule (labelled

¹ Throughout this work, we adopt a system of units where $\hbar = 1$.

D) formed by the two atoms A_1 and A_2 of masses m_1 and m_2 respectively, with $m_1 < m_2$, then has a weakly bound state of binding energy $E_D = 1/(2\mu a^2)$, where $\mu = m_1 m_2 / (m_1 + m_2)$. The elastic scattering phase shift, $\delta_{A_2 D}^{(J)}(k_E)$, for the scattering of atom A_2 by the diatomic molecule D at angular momentum J and $k_E = \sqrt{2\mu_{A_2 D}(E + E_D)}$, where E is the three-body energy, is given by

$$\mathcal{A}_J(k_E, k_E; E, \Lambda) = \frac{2\pi}{\mu_{A_2 D}} \frac{1}{k_E \cot \delta_{A_2 D}^{(J)}(k_E) - ik_E}. \quad (2)$$

Here, $\mu_{A_2 D} = m_2(m_1 + m_2)/(2m_2 + m_1)$ is the reduced mass of the $A_2 D$ system, and the on-shell scattering amplitude, $\mathcal{A}_J(k_E, k_E; E, \Lambda)$, can be obtained by solving the modified STM equation [20, 30]

$$\begin{aligned} \mathcal{A}_J(p, k; E, \Lambda) &= \frac{2\pi m_1}{a\mu^2} (-1)^n M_J(p, k; E) \\ &+ \frac{m_1}{\pi\mu} \int_0^\Lambda dq q^2 M_J(p, q; E) \frac{(-1)^n \mathcal{A}_J(q, k; E, \Lambda)}{-1/a + \sqrt{-2\mu(E - q^2/(2\mu_{A_2 D}))} - i\epsilon}. \end{aligned} \quad (3)$$

The kernel function $M_J(p, q; E)$, which can be interpreted as the potential generated by the exchange of the light atom in partial wave J , is given by

$$M_J(p, q; E) = \frac{1}{pq} Q_J \left(\frac{p^2 + q^2 - 2\mu E - i\epsilon}{2pq\mu/m_1} \right), \quad (4)$$

where $Q_J(z)$ are the Legendre functions of the second kind, which can be written in terms of the Legendre polynomials of order J as

$$Q_J(z) = \frac{1}{2} \int_{-1}^1 dx \frac{P_J(x)}{z - x}. \quad (5)$$

The integer n in Eq. (3) is equal to J if the heavy particle is bosonic and $J + 1$ if it is fermionic. In this work, we focus on the bosonic case, which is more relevant for current experiments. For $J \geq 1$, the solutions of Eq. (3), and consequently the phase shifts obtained from Eq. (2), are independent of Λ as long as $p, k, 1/a \ll \Lambda$ and $m_2/m_1 < 38.63$, beyond which the D-wave Efimov effect enters [31, 32]. We restrict ourselves to these limits in this work.

However, for $J = 0$, the scattering amplitude in Eq. (3), while finite, does not converge as $\Lambda \rightarrow \infty$. In this scenario, there is a linear relationship between the cutoff Λ and the three-body parameter, κ_*^2 , resulting in a log-periodicity of the amplitude in the cutoff with a period equal to the system-dependent scaling factor λ [28, 33, 34]. By solving the STM equation for various Λ values in the range $1/a \ll \Lambda_0 < \Lambda < \lambda\Lambda_0$ for some Λ_0 , we obtain a set of phase shifts $\delta_{A_2 D}^{(0)}(k_E)$ corresponding to various values of κ_* . As we discuss later in Sec. III, the Efimov radial law is then fit to these phase shifts in order to obtain universal scaling functions that are cutoff independent.

The kernel of the STM equation has a branch cut in the complex q -plane for energies above the three-atom threshold. To circumvent it, we rotate the integration path by an angle ϕ into the fourth quadrant and integrate along a straight line from the origin to $\Lambda e^{-i\phi}$ [35]. Unlike in Ref. [35], though, it is important to include the contribution from the arc connecting $\Lambda e^{-i\phi}$ and Λ to obtain correct values for the cutoff dependent amplitudes.

III. RECOMBINATION RATES AND SCALING FUNCTIONS

A. Rate Constant and Threshold Behavior

A system of three atoms ($A_1 A_2 A_2$), consisting of two atoms of species 2 with atomic number density n_2 and one atom of species 1 with number density n_1 , in a shallow trap can leave the trap as an $A_2 D$ pair by undergoing a three-body recombination process. For the $A_1 A_2 A_2$ system, the recombination rate constant α is defined by

$$\frac{d}{dt} n_2 = 2 \frac{d}{dt} n_1 = -2\alpha n_1 n_2^2. \quad (6)$$

² One may alternatively consider $1/a_{*0}$, the location of a recombination minimum, as a three-body parameter.

At $E = 0$, the rate constant, α_s , for recombination into a shallow-bound diatomic molecular state with binding energy E_D can be numerically evaluated from the A_2D scattering amplitude using [20, 24]

$$\alpha_s = 4\mu_{A_2D} \sqrt{\frac{\mu_{A_2D}}{\mu}} a^2 \left| \mathcal{A}_0 \left(0, \frac{1}{a} \sqrt{\frac{\mu_{A_2D}}{\mu}}; 0 \right) \right|^2. \quad (7)$$

Its dependence on the scattering length a is given by the analytic expression [20]

$$\alpha_s = C(\delta) \frac{\sin^2 \theta_{*0} + \sinh^2 \eta_*}{\sinh^2(\pi s_0 + \eta_*) + \cos^2 \theta_{*0}} \frac{a^4}{m_1}. \quad (8)$$

The explicit dependence on the mass ratio $\delta = m_1/m_2$ is captured by the coefficient

$$C(\delta) = 64\pi^2 \left[(1 + \delta^2)\phi(\delta) - \sqrt{\delta(2 + \delta)} \right], \quad (9)$$

where the phase $\phi(\delta) = \arcsin[(1 + \delta)^{-1}]$, and the scaling factor s_0 is the solution of the transcendental equation

$$s_0 \cosh[\pi s_0/2] \sin[2\phi(\delta)] - 2 \sinh[s_0\phi(\delta)] = 0. \quad (10)$$

The angle θ_{*0} is given by

$$\theta_{*0} = s_0 \ln(a/a_{*0}), \quad (11)$$

where a_{*0} is the value of the scattering length a at a recombination minimum, and it follows that Eq. (8) is a log-periodic function of a with the period $\lambda = e^{\pi/s_0}$. The inelasticity parameter η_* is introduced by analytically continuing the real-valued θ_{*0} to the complex value $\theta_{*0} + i\eta_*$, which is formally equivalent to introducing an anti-Hermitian term in the three-body Hamiltonian [36, 37]. This is done to take into account the modification of α_s by the existence of deeply bound diatomic molecular states, which are frequently present in experimental systems. The value of a_{*0} that corresponds to a particular cutoff is determined by fitting the expression in Eq. (8) to the numerical results obtained from Eq. (7) for $\eta_* = 0$ over a range of a values. This gives us the proportional relationship between Λ and $1/a_{*0}$ [3] needed for the extraction of the universal scaling functions.

Additionally, there is a direct contribution to the total three-body recombination rate constant α due to the formation of deeply bound diatomic molecules in the final state. The threshold expression for this contribution is given by [20]

$$\alpha_d = C(\delta) \frac{\coth(\pi s_0) \cosh(\eta_*) \sinh(\eta_*)}{\sinh^2(\pi s_0 + \eta_*) + \cos^2 \theta_{*0}} \frac{a^4}{m_1}. \quad (12)$$

The maximum threshold value of the recombination rate constant, α_{th}^{max} , is the sum of the maxima of both the shallow and deep molecule rate constants, which occur at $\theta_{*0} = \pi/2$, and is

$$\alpha_{th}^{max} = C(\delta) \frac{1 + \sinh^2 \eta_* + \coth(\pi s_0) \cosh(\eta_*) \sinh(\eta_*)}{\sinh^2(\pi s_0 + \eta_*)} \frac{a^4}{m_1}. \quad (13)$$

Equations (8), (12) and (13) provide a useful check for our three-body recombination rate at non-zero energy, $K_3^{(J)}(E)$, defined below.

B. Three-body Recombination and Universal Scaling Functions

The three-body recombination rate at energy E , $K_3^{(J)}(E)$, is related to the S-matrix for the inelastic $A_1A_2A_2 \rightarrow A_2D$ scattering process. However, through the unitarity of the total S-matrix that includes both elastic and inelastic contributions, we can write the recombination rate purely in terms of the S-matrix for elastic A_2D scattering, $S_{A_2D,A_2D}^{(J)}(E) = \exp[2i\delta_{A_2D}^{(J)}(E)]$ [25], as

$$K_3^{(J)}(E) = \frac{128\pi^2 \mu^{3/2}}{\mu_{A_2D}^{3/2}} \frac{(2J+1)}{x^4} \left(1 - |S_{A_2D,A_2D}^{(J)}(E)|^2 \right) \frac{a^4}{2\mu}, \quad (14)$$

where the dimensionless scaling variable x is $\sqrt{E/E_D}$. This relation is valid in the absence of deeply bound molecules, the effects of which we take into account later in this subsection. The detailed derivation of Eq. (14) is given in App. A.

1. $J \geq 1$:

For each total orbital angular momentum $J \geq 1$, there is one corresponding real-valued scaling function

$$f_J(x) = 1 - e^{-4\text{Im}\delta_{A_2D}^{(J)}(E)}, \quad (15)$$

which allows us to obtain the J^{th} partial-wave contribution to the three-body recombination rate. Generally, only the first few J values are expected to be necessary before additional contributions to the total rate become negligible. As we increase the value of J , the numerical method used to calculate the phase shifts with which we find $f_J(x)$ loses accuracy at small values of x , and we need to use the approximate form

$$f_J(x) \approx a_J x^{2\lambda_J+4} + b_J x^{2\lambda_J+6}, \quad (16)$$

for small x , where $\lambda_J = J$ [25, 38], and the coefficients a_J and b_J are obtained by fitting Eq. (16) to $f_J(x)$ data at low x -values with small numerical uncertainties.

The energy-dependent three-body recombination rate $K_3^{(J \geq 1)}(E)$ is then given by

$$K_3^{(J \geq 1)}(E) = \frac{128\pi^2 \mu^{3/2}}{\mu_{A_2D}^{3/2}} \frac{(2J+1)f_J(x)}{x^4} \frac{a^4}{2\mu}. \quad (17)$$

2. $J = 0$:

In the $J = 0$ channel, the elements of the S-matrix for elastic A_2D scattering are related to universal functions s_{ij} of the scaling variable x using Efimov's Radial Law [3],

$$S_{A_2D, A_2D}^{(J=0)}(E) = s_{22}(x) + \frac{s_{21}(x)^2 e^{2i\theta_{*0}-2\eta_*}}{1 - s_{11}(x)e^{2i\theta_{*0}-2\eta_*}}. \quad (18)$$

We obtain the complex-valued scaling functions $s_{ij}(x)$ by temporarily setting $\eta_* = 0$ and fitting Eq. (18) for each x to numerical values of phase shifts obtained from Eqs. (2) and (3) for the range of a_{*0} generated by varying Λ as discussed in Sec. II. The S-wave scaling functions of the form $|s_{ij}|e^{i\theta_{ij}}$ for ^{40}K - ^{87}Rb , ^6Li - ^{87}Rb , ^{40}K - ^{133}Cs , and ^6Li - ^{133}Cs are shown in Fig. 1. Values for η_* have been determined or estimated in either experiments or theoretical calculations for these systems [20, 26, 39, 40] and are included in the S-wave three-body recombination rate for shallow and deep diatomic molecules.

With the universal functions s_{ij} , we can calculate the S-wave heteronuclear three-body recombination rate $K_3^{(0)}(E)$ from

$$K_3^{(0)}(E) = \frac{128\pi^2 \mu^{3/2}}{\mu_{A_2D}^{3/2}} \frac{1}{x^4} \left(1 - \left| s_{22}(x) + \frac{s_{12}(x)^2 e^{2i\theta_{*0}-2\eta_*}}{1 - s_{11}(x)e^{2i\theta_{*0}-2\eta_*}} \right|^2 - \frac{(1 - e^{-4\eta_*}) |s_{12}(x)|^2}{|1 - s_{11}(x)e^{2i\theta_{*0}-2\eta_*}|^2} \right) \frac{a^4}{2\mu}, \quad (19)$$

where the third term in parenthesis in Eq. (19) arises from incorporating possible transitions from an A_2D scattering state or three-atom scattering state into an atom and a deeply bound diatomic molecule in the intermediate state. To obtain results for a given system, we take the position of one of the recombination minima as an experimental or theoretical input for that system.

There is an additional contribution from the formation of deeply bound molecules in the final state, whose significance for a particular system depends on the size of η_* . These effects are subleading in the zero-range limit for $J \geq 1$ [25]. However, for $J = 0$, the contribution,

$$K_3^{deep}(E) = \frac{128\pi^2 \mu^{3/2} (1 - e^{-4\eta_*}) \left(1 - |s_{11}(x)|^2 - |s_{12}(x)|^2 \right) a^4}{\mu_{A_2D}^{3/2} x^4 |1 - s_{11}(x)e^{2i\theta_{*0}-2\eta_*}|^2} \frac{a^4}{2\mu}, \quad (20)$$

appears at leading order and must be added to the rate of recombination into shallow diatomic molecules in order to obtain the full recombination rate.

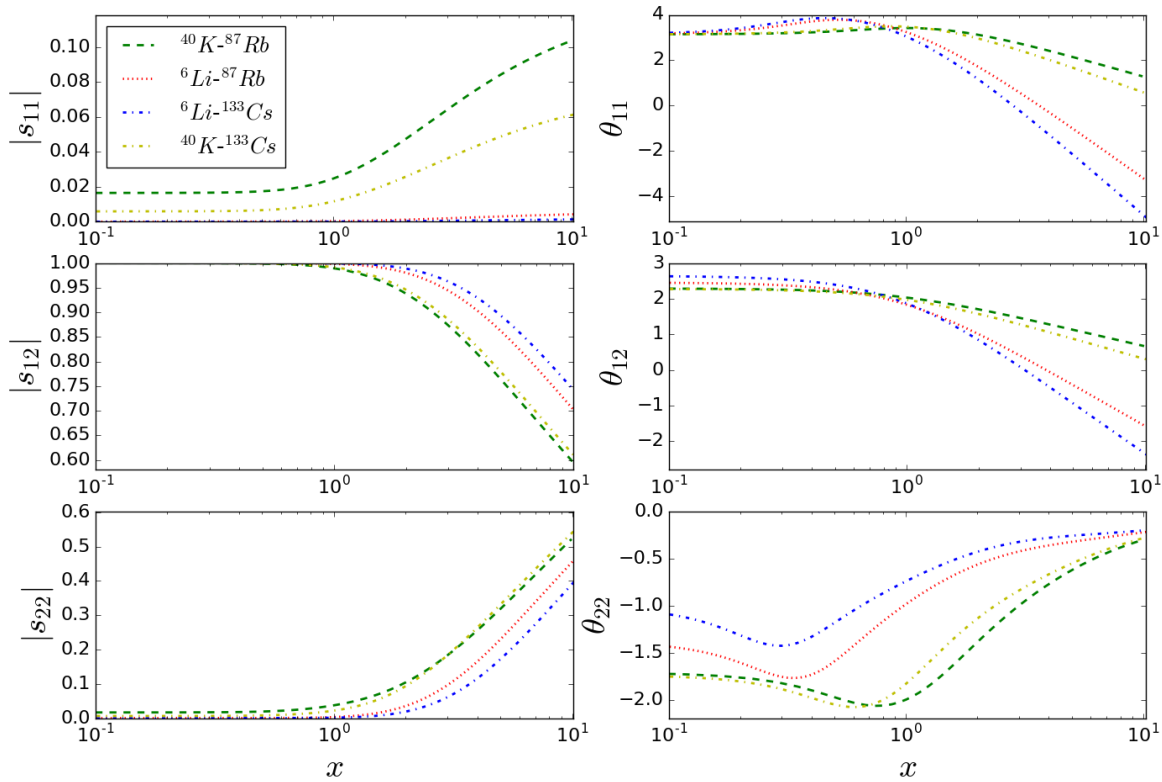


FIG. 1: S-wave universal functions for $^{40}\text{K-}^{87}\text{Rb}$, $^{40}\text{K-}^{133}\text{Cs}$, $^6\text{Li-}^{87}\text{Rb}$, and $^6\text{Li-}^{133}\text{Cs}$.

We have checked and verified the $E \rightarrow 0$ limits of $K_3^{(0)}(E)$ and $K_3^{deep}(E)$ given by Eqs. (19) and (20) by comparing them to the corresponding threshold expressions given by Eqs. (8) and (12) multiplied by a factor of 2 that comes from the statistics of the system. The total threshold S-wave recombination rate containing the contribution of both shallow and deep states, $K_3^{(0)}(0) + K_3^{deep}(0)$, has a maximum value of K_{th}^{max} at $\theta_{*0} = \pi/2$. This is related to α_{th}^{max} defined in Eq. (13) by the relation $K_{th}^{max} = 2\alpha_{th}^{max}$.

In Fig. 2, we plot the energy dependence of $K_3^{(0)}(E)$ and $K_3^{deep}(E)$ at various values of θ_{*0} for the $^{40}\text{K-}^{87}\text{Rb}$ and $^6\text{Li-}^{87}\text{Rb}$ systems³. The rates are expressed in the units of K_{th}^{max} . The variations in the shape of the $K_3^{(0)}(E)$ curves by up to several orders of magnitude as θ_{*0} varies show that the energy dependence of S-wave recombination into a shallow diatomic molecular state has an intricate dependence itself on the scattering length a and the scaling parameter s_0 .

Figure 3 shows the energy dependence of $K_3^{(J \geq 1)}(E)$ for the $^{40}\text{K-}^{87}\text{Rb}$ and $^6\text{Li-}^{87}\text{Rb}$ systems. These are expressed in the units of the threshold S-wave rate maximum, K_{th}^{max} . For the $^{40}\text{K-}^{87}\text{Rb}$ system, we observe diminishing contributions as we go to higher partial waves. This is different from the behavior of a system of three identical bosons, in which the contribution of the $J = 1$ partial wave was found to be comparable to that of the $J = 4$ partial wave [25]. The near-threshold energy dependence of the recombination rates $K_3^{(J)}(E)$ in Figs. 2 and 3 agrees with the predictions given in Ref. [41]. However, we do not reproduce the dependence on the mass ratio δ suggested by Ref. [41].

Comparing Figs. 2 and 3 informs us about the temperature scale around and above which the recombination minima are unlikely to be measured due to large partial wave contributions. In $^{40}\text{K-}^{87}\text{Rb}$, the $J = 1$ partial wave becomes larger than the S-wave around E_D and the corresponding temperature is $T_{\text{KRb}} = 0.3E_D/k_B \approx 0.1(a/a_0)^{-2} \text{K}$, where

³ Numerical data for these and other systems can be provided by the authors on request.

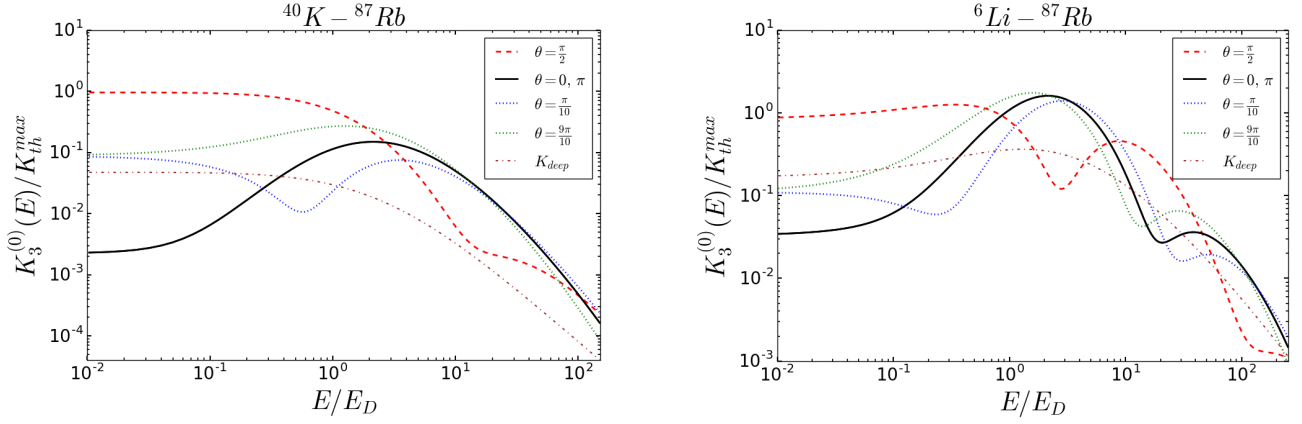


FIG. 2: Left panel: The $J = 0$ recombination rate divided by the maximum threshold value, K_{th}^{max} , for a variety of values of θ_{*0} in the $^{40}\text{K}-^{87}\text{Rb}$ system with $\eta_* = 0.05$. Right panel: The $J = 0$ recombination rate divided by the maximum threshold value, K_{th}^{max} , for a variety of values of θ_{*0} in the $^6\text{Li}-^{87}\text{Rb}$ system with $\eta_* = 0.2$.

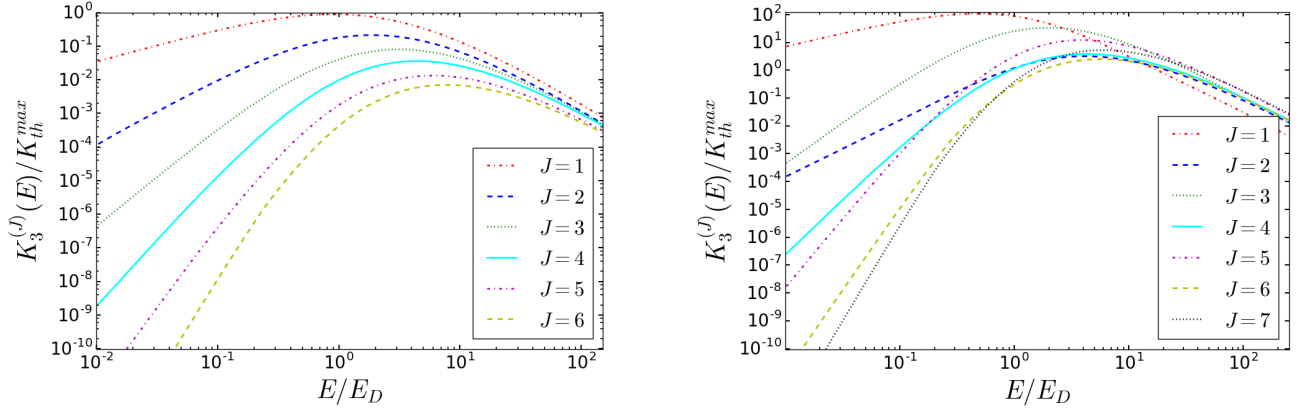


FIG. 3: Left panel: $K_3^{(J)}(E)/K_{th}^{max}$ for $^{40}\text{K}-^{87}\text{Rb}$. Right panel: $K_3^{(J)}(E)/K_{th}^{max}$ for $^6\text{Li}-^{87}\text{Rb}$.

a_0 is the Bohr radius. On the other hand, in the $^6\text{Li}-^{87}\text{Rb}$ system it happens at a very low energy $\sim 10^{-3}E_D$, which corresponds to the temperature $T_{\text{LiRb}} = 10^{-3}E_D/k_B \approx 0.015(a/a_0)^{-2}\text{K}$. These relations either give a maximum scattering length below which the minima can be observed, provided that the universal region $a \gg \ell$ still exists, or set a target temperature below which we may begin to observe known minima around the value of a and below.

IV. COMPARISON WITH EXPERIMENT

To make a comparison of our results with experiments we require input values for a_{*0} and η_* . We calculate the contributions from all different scattering sectors and combine them into a total recombination rate,

$$K_3(E) = \sum_{J=0}^{\infty} K_3^{(J)}(E) + K_3^{deep}(E). \quad (21)$$

We then perform a thermal average over $K_3(E)$ to obtain the recombination rate constant for a specific scattering length at a finite temperature used in relevant experiments [25],

$$\alpha_T \approx \frac{\int_0^{\infty} dE E^2 e^{-E/(k_B T)} K_3(E)}{2 \int_0^{\infty} dE E^2 e^{-E/(k_B T)}}, \quad (22)$$

where the coefficient 2 in the denominator is the symmetry factor.

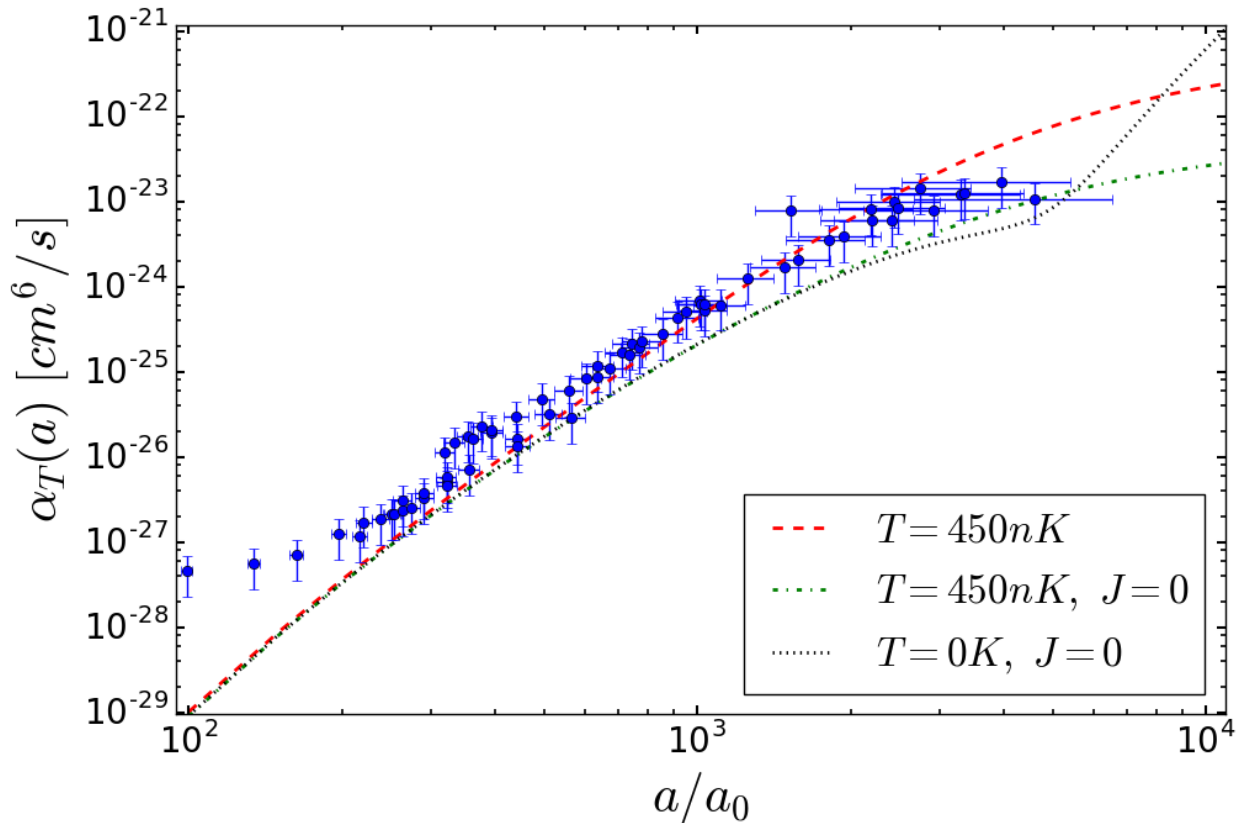


FIG. 4: The recombination rate constant α_T as a function of the scattering length a for ^{40}K - ^{87}Rb with $\eta_* = 0.05 \pm 0.02$ [20] and the three-body parameter adjusted to reproduce a recombination minimum at $a_{*0} \approx 5000a_0$. The dashed red line at 450 nK corresponds to the average temperature at which the data of Bloom *et al.* was taken [39].

The inelasticity parameter for a ^{40}K - ^{87}Rb mixture was estimated by Bloom *et al.* [39] to be $\eta_* = 0.26$ by matching a threshold formula for the atom-molecule relaxation loss rate coefficient β to experimental data. But, they later gave $\eta_* = 0.02$ as a good match for their measurements of the rate constant α . The published data, though, is restricted to a values smaller than the thermal wavelength of the atoms set by the temperature of the gas in the experiment. Meanwhile, Helfrich, Hammer, and Petrov find $\eta_* = 0.05 \pm 0.02$ [20] by fitting their Eq. (20) to the corresponding data from Ref. [42]. We use the experimental value $a_* = 230 \pm 30a_0$ obtained in Ref. [39] for ^{40}K - ^{87}Rb to determine the position of the recombination minimum $a_{*0} \approx 5000a_0$. We achieve this by employing the ^{40}K - ^{87}Rb universal relation $a_*/a_{*0} = 0.51 \exp(\pi/(2s_0))$ [20], which is exact in the zero-range limit employed in this work. Here, a_* is the value of a where the Efimov trimer state reaches the A_2D threshold. On the other hand, Wang *et al.* [22] predicted from a theoretical calculation that $a_{*0} = 2800a_0$. In their procedure to obtain this value, they set the Rb-Rb scattering length to $a_{22} = 100a_0$. The relatively large temperatures used in the experiment by Bloom *et al.* do not allow for the observation of this feature. Therefore, the discrepancy between the universal prediction obtained from the value of a_* and the result presented in Ref. [22] cannot be addressed. We find that a temperature of approximately 10 nK would be necessary to clearly observe recombination minima in this experiment.

Bloom *et al.* also gave evidence that we can neglect the ^{87}Rb - ^{87}Rb - ^{87}Rb recombination channel due to the small scattering length a_{22} , with an observed ratio of ^{87}Rb loss to ^{40}K loss of 2.1(1) indicating that the dominant loss channel is ^{40}K - ^{87}Rb - ^{87}Rb recombination. We also note that the uncertainty introduced by neglecting the small scattering length a_{22} in the calculation of ^{40}K - ^{87}Rb - ^{87}Rb recombination rate is of the order of a_{22}/a . The perturbative approach introduced in Ref. [24] could be employed to account for such corrections as long as $a_{22} < a$.

Further, though we use the value of $a_{*0} \approx 5000a_0$ for the position of a recombination minimum, this minimum was

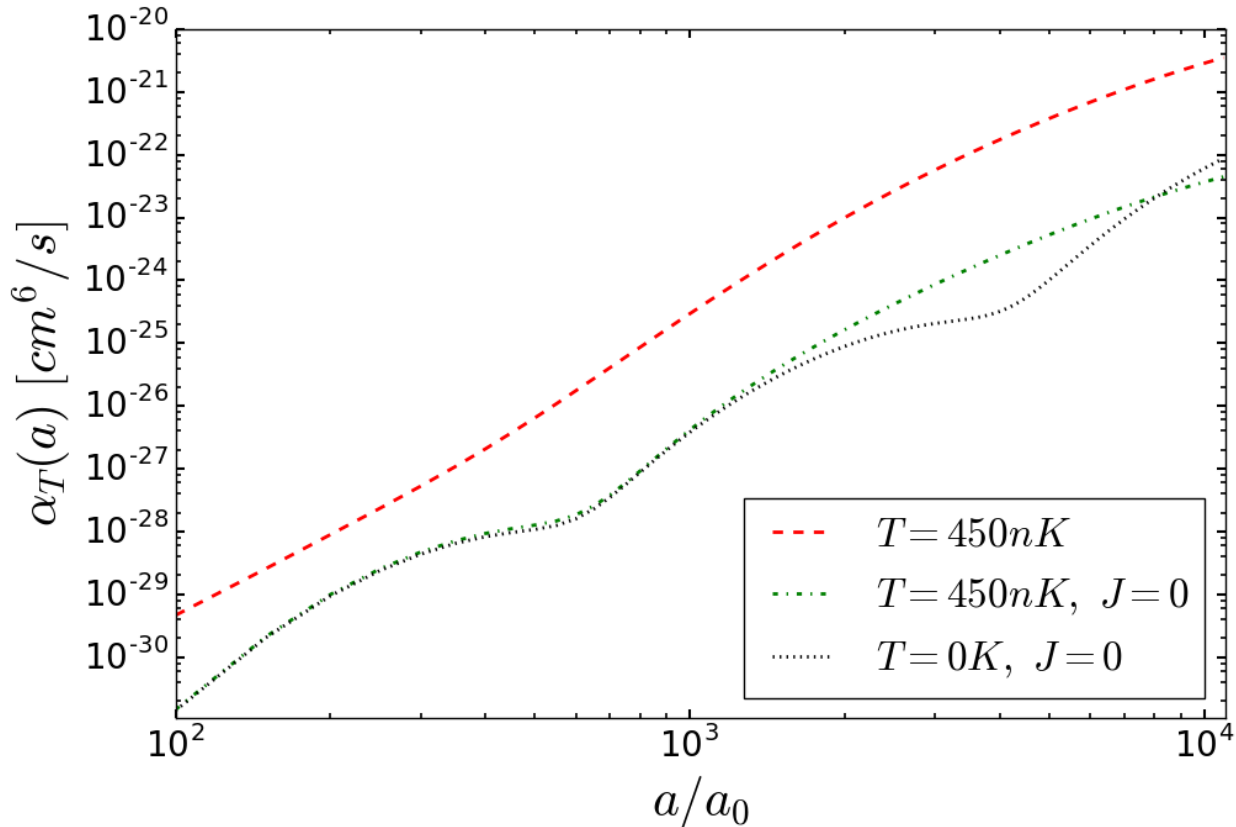


FIG. 5: The recombination rate constant α_T as a function of the scattering length a for ${}^6\text{Li}-{}^{87}\text{Rb}$ for $\eta_* = 0.2$ [26] with a recombination minimum at $a_{*0} \approx 610a_0$.

not probed in Ref. [39], since they were limited by their experimental temperature of $T \sim 300\text{ nK}$ to $a \lesssim 3000a_0$.⁴ Experimental uncertainties become quite large near and beyond this value. This means that for ${}^{40}\text{K}-{}^{87}\text{Rb}$ no Efimov features were definitively observed for three-body recombination in currently accessed positive scattering lengths. In Fig. 4, we show the data of Ref. [39] and our numerically obtained curves for rate constant α_T , with one curve showing the $J = 0$ contribution to the rate constant and another showing the total rate after summing over J . We also include the zero temperature result obtained by summing Eqs. (8) and (12) for comparison. In each of our curves in the figure we have selected $a_{*0} = 5000a_0$ and $\eta_* = 0.05$. The agreement of the 450 nK curve with the experimental data is excellent in the large a region where the neglected contributions due to finite range and finite a_{22} corrections become small [24]. The size of the discrepancy at $a \lesssim 200a_0$ suggests that the latter might perhaps be more important for this experiment than the former, since, with a quoted value of the van der Waals' range $R_{vdW} = 72a_0$ [39], range corrections are expected to be about 35%-70% in this region. Our results at lower temperatures indicate the minima at $5000a_0$ can only be observed at temperatures well below 10 nK, which may not be experimentally feasible.

The similar ${}^{39}\text{K}-{}^{87}\text{Rb}$ and ${}^{41}\text{K}-{}^{87}\text{Rb}$ systems were studied by Wacker *et al.* [43]. For $a > 0$, no signatures of Efimov resonances were seen in either mixture for accessible scattering lengths and temperatures, further demonstrating how a large scaling factor makes the observation of universality difficult and giving a compelling argument in favor of using systems with a larger mass imbalance such as ${}^6\text{Li}-{}^{87}\text{Rb}$ or ${}^6\text{Li}-{}^{133}\text{Cs}$. We therefore study the effects of temperature on the recombination rate constant for the ${}^6\text{Li}-{}^{87}\text{Rb}$ system in Fig. 5. We examine a couple of different sources to obtain inputs for a_{*0} and η_* . First, the ${}^7\text{Li}-{}^{87}\text{Rb}$ system was studied by Maier *et al.* in Ref. [44], and they found a value of $|a_-| = 1870 \pm 121a_0$. They further suggest a value of a_- of $-1600a_0$ for ${}^6\text{Li}-{}^{87}\text{Rb}$, which, with $|a_-|/a_{*0} = \exp(\pi/2s_0)$, gives a recombination minimum position of $a_{*0} \approx 610a_0$. Additionally, for ${}^6\text{Li}-{}^{87}\text{Rb}$, Petrov and Werner, in the absence of any known experimental results, give $\eta_* = 0.2$ [26]. We adopt the use of $\eta_* = 0.2$ and $a_{*0} = 610a_0$ in

⁴ Although the average temperature for their experiment was around 450 nK, the data at the largest a values was taken near 300 nK.

Fig. 5. We find that the recombination minima are obscured by the finite temperature effects, particularly by the ones that enter in partial waves $J \geq 1$, though even for the $J = 0$ (dot-dashed) line the second minimum is obscured. The effects of higher partial waves begin to be suppressed below ~ 10 nK, and the minimum at $610a_0$ becomes accessible in experiments. We have performed the partial wave analysis shown earlier in Fig. 3 for several systems and found that higher partial wave contributions become increasingly dominant at smaller m_1/m_2 . Therefore, in order to see the detailed universal behavior, it appears that one must prepare the system at very low temperatures for small mass ratios. Illustrative plots of the recombination rate constant for two additional systems beyond those shown above are given in App. B.

This trend stands in contrast to the suggestion of D’Incao and Esry [41] that the dominant contribution to recombination in systems in which A_2 is bosonic comes from the $J = 0$ channel. While this is certainly true when $E = 0$, it does not appear to be true at all values of E , particularly for systems with small m_1/m_2 .

V. CONCLUSION

In this work, we considered three-body recombination in heteronuclear systems with positive interspecies scattering length at finite temperature. Using the STM equation, we obtained sets of universal scaling functions that can be used to calculate the temperature dependent recombination rate for arbitrary values of the three-body parameter and inelasticity parameter η_* . Every mass ratio requires a new set of scaling functions and we calculated these for various systems of interest. We also calculated the universal scaling functions for higher partial waves that do not display the Efimov effect but contribute to the total loss rate. Our results show that observing the Efimov effect becomes difficult due to relatively large recombination rate contributions from higher partial wave scattering channels at experimentally feasible temperatures. This obfuscation of S-wave universality becomes particularly acute for systems with small m_1/m_2 , and reduces their favorability for the experimental observation of Efimov features when $a > 0$. We have compared our results with experimental results for three-body combination in an ultracold mixture of ^{40}K - ^{87}Rb atoms and found good agreement with the data.

In future work, we will address the impact of corrections due to the finite range of the interactions. These effects were studied in the framework of effective field theory for identical bosons in Refs. [29, 45] and for heteronuclear systems in Ref. [24]. Including range corrections to the temperature-dependent three-body recombination process will enable us to understand Efimov physics even when a is not particularly large and might help us avoid the range of a values where higher partial wave contributions are dominant. The effects of a finite intraspecies scattering length a_{22} have been incorporated perturbatively [24] for $|a_{22}| \ll |a|$ and $T = 0$ K and nonperturbatively [26] for $|a_{22}| \sim |a|$ at finite T for $a < 0$. But, this remains to be done for finite T when $a > 0$. Major extensions to the existing formalism will be required to accommodate additional scattering channels if $a_{22} > 0$.

Acknowledgments

We thank Ruth Bloom for providing us with the recombination data of Ref. [39] and Eric Braaten for comments on the manuscript. This work was supported by the U.S. Department of Energy through the Office of Science, Office of Nuclear Physics under Contract Nos. DE-AC52-06NA25396, DE-AC05-00OR22725, an Early Career Research Award, the LANL/LDRD Program, and by the National Science Foundation under Grant No. PHY-1555030.

Appendix A: Phase Space Factors

We calculate the three-body recombination rate by relating it to the cross section for inelastic A_2D scattering, $\sigma_{A_2D}^{(\text{inelastic})}$. This cross section is defined as

$$\sigma_{A_2D}^{(\text{inelastic})} = \frac{1}{2v_{A_2D}} |\mathcal{A}_{A_2D, A_1 A_2 A_2}|^2 \Phi_3, \quad (\text{A1})$$

where $\mathcal{A}_{A_2D, A_1 A_2 A_2}$ denotes the amplitude for a transition from an A_2D state to three atoms, the relative velocity of the atom A_2 and molecule D is $v_{A_2D} = k_E/\mu_{A_2D}$ and $k_E = \sqrt{2\mu_{A_2D}(E + E_D)}$, and the flux factor Φ_3 is the three-body phase space. We also include a symmetry factor of 2 into the expression for the total cross section since we have 2 identical particles in the final state.

Further, one can write the three-body recombination rate K_3 as

$$K_3 = |\mathcal{A}_{A_1 A_2 A_2, A_2 D}|^2 \Phi_2 = 2v_{A_2 D} \frac{\Phi_2}{\Phi_3} \sigma_{A_2 D}^{(\text{inelastic})}. \quad (\text{A2})$$

The inelastic cross section can be rewritten in terms of total and elastic ones as

$$\begin{aligned} \sigma_{A_2 D}^{(\text{inelastic})} &= \sigma_{A_2 D}^{(\text{tot})} - \sigma_{A_2 D}^{(\text{elastic})} \\ &= (2J+1) \left[\frac{2\mu_{A_2 D}}{k_E} \text{Im} A_J(k_E, k_E, E) - \frac{\mu_{A_2 D}^2}{\pi} |A_J(k_E, k_E, E)|^2 \right] \\ &= (2J+1) \frac{\pi}{k_E^2} \left[1 - \left| e^{2i\delta_{A_2 D}^{(J)}(E)} \right|^2 \right], \end{aligned} \quad (\text{A3})$$

where we used Eq. (2) to arrive at the last line. This relates the recombination rate to the phase shift (*i.e.* the S-matrix element) given in Eq. (14) with a normalization factor determined by the ratio Φ_2/Φ_3 .

The two-body phasespace Φ_2 is given by

$$\begin{aligned} \Phi_2 &= \int \frac{d^3 p_A}{(2\pi)^3} \frac{d^3 p_D}{(2\pi)^3} (2\pi)^3 \delta^{(3)}(p_A + p_D) 2\pi \delta \left(E - \frac{p_A^2}{2m_2} - \frac{p_D^2}{2(m_1 + m_2)} + E_D \right) \\ &= \frac{\mu_{A_2 D} k_E}{\pi}. \end{aligned} \quad (\text{A4})$$

The three-atom final state phasespace factor is

$$\begin{aligned} \Phi_3 &= \int \prod_{i=1}^3 \frac{d^3 p_i}{(2\pi)^3} (2\pi)^3 \delta^{(3)}(\mathbf{p}_1 + \mathbf{p}_2 + \mathbf{p}_3) 2\pi \delta \left(E - \frac{p_1^2}{2m_1} - \frac{p_2^2}{2m_2} - \frac{p_3^2}{2m_2} \right) \\ &= \frac{(\mu\mu_{A_2 D})^{3/2}}{8\pi^2} E^2, \end{aligned} \quad (\text{A5})$$

where the \mathbf{p}_i 's, with $i = 1, 2, 3$, denote the momenta of the three final state atoms. Using these phasespace factors in Eq. (A2) leads to the final result

$$K_3 = \frac{16\pi^2}{(\mu\mu_{A_2 D})^{3/2} E^2} (2J+1) \left[1 - \left| e^{2i\delta_{A_2 D}^{(J)}} \right|^2 \right]. \quad (\text{A6})$$

Making the substitution $E = x^2/(2\mu a^2)$ leads to Eq. (14).

Appendix B: Additional Systems

A few additional systems have been studied in order to facilitate a broader understanding of the significance of higher partial wave contributions to the three-body recombination rate across a range of A_1 - A_2 mass ratios, and the rates for two of these are presented in Fig. 6. Lacking known values for the three-body and inelasticity parameters in the ^{40}K - ^{133}Cs system, we set $a_{*0} = 500a_0$ and $\eta_* = 0.2$. For ^6Li - ^{133}Cs , we use the three-body parameter $a_{*0} \approx 805a_0$ obtained from the value $a_- = -1777a_0$ [40] via the universal relation between the two parameters. In Ref. [40], values for η_* were estimated at 120 nK and 450 nK and are given by $\eta_*^{(120)} = 0.61$ and $\eta_*^{(450)} = 0.86$, respectively. For our purposes, we set $\eta_* = 0.2$ for this system in order to clearly show locations of minima and the effects of finite temperature and higher partial wave contributions. The two plots in Fig. 6 further illustrate the trend that systems with more extreme mass ratios experience larger $J \geq 1$ recombination rate contributions.

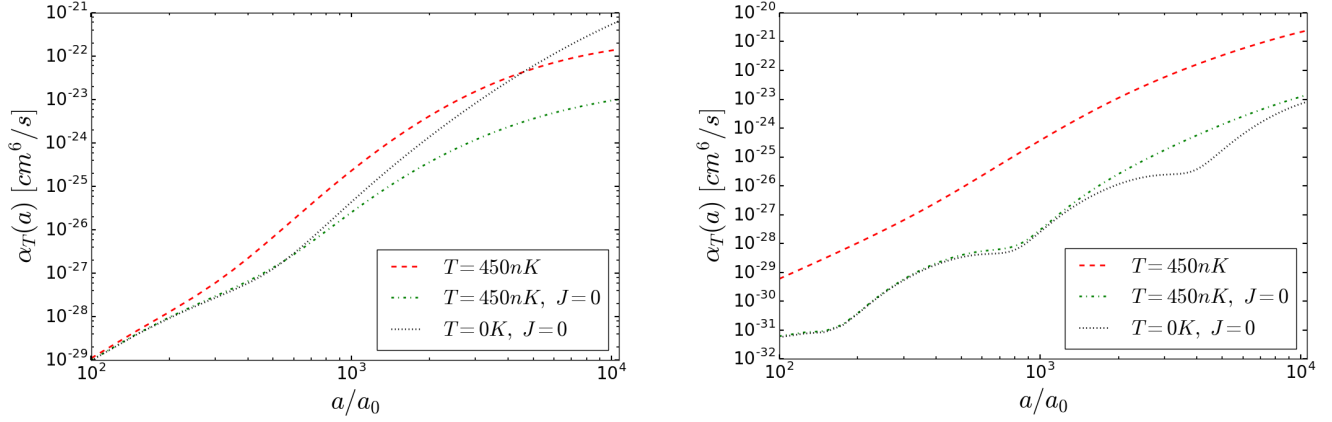


FIG. 6: Left panel: Rate constant $\alpha_T(a)$ for ^{40}K - ^{133}Cs , with $a_{*0} = 500a_0$ and $\eta_* = 0.2$. Right panel: Rate constant $\alpha_T(a)$ for ^6Li - ^{133}Cs , with $a_{*0} = 805a_0$ [40] and $\eta_* = 0.2$.

-
- [1] H.-W. Hammer and L. Platter, *Annu. Rev. Nucl. Part. Sci.* **60**, 207 (2010).
[2] V. Efimov, *Phys. Lett.* **33B**, 563 (1970).
[3] E. Braaten and H.-W. Hammer, *Phys. Rept.* **428**, 259 (2006).
[4] T. Kraemer, M. Mark, P. Waldburger, J. G. Danzl, C. Chin, B. Engeser, A. D. Lange, K. Pilch, A. Jaakkola, H.-C. Nägerl, et al., *Nature* **440**, 315 (2006).
[5] N. Gross, Z. Shotan, S. Kokkelmans, and L. Khaykovich, *Phys. Rev. Lett.* **103**, 163202 (2009).
[6] S. E. Pollack, D. Dries, and R. G. Hulet, *Science* **326**, 1683 (2009).
[7] N. Gross, Z. Shotan, S. Kokkelmans, and L. Khaykovich, *Phys. Rev. Lett.* **105**, 103203 (2010).
[8] T. B. Ottenstein, T. Lompe, M. Kohnen, A. N. Wenz, and S. Jochim, *Phys. Rev. Lett.* **101**, 203202 (2008).
[9] J. H. Huckans, J. R. Williams, E. L. Hazlett, R. W. Stites, and K. M. O'Hara, *Phys. Rev. Lett.* **102**, 165302 (2009).
[10] J. R. Williams, E. L. Hazlett, J. H. Huckans, R. W. Stites, Y. Zhang, and K. M. O'Hara, *Phys. Rev. Lett.* **103**, 130404 (2009).
[11] S. Floerchinger, R. Schmidt, and C. Wetterich, *Phys. Rev. A* **79**, 053633 (2009).
[12] P. Naidon and M. Ueda, *Phys. Rev. Lett.* **103**, 073203 (2009).
[13] E. Braaten, H.-W. Hammer, D. Kang, and L. Platter, *Phys. Rev. Lett.* **103**, 073202 (2009).
[14] E. Braaten, H.-W. Hammer, D. Kang, and L. Platter, *Phys. Rev. A* **81**, 013605 (2010).
[15] H.-W. Hammer, D. Kang, and L. Platter, *Phys. Rev. A* **82**, 022715 (2010).
[16] P. Naidon and S. Endo, *Rep. Prog. Phys.* **80**, 056001 (2017).
[17] G. Barontini, C. Weber, F. Rabatti, J. Catani, G. Thalhammer, M. Inguscio, and F. Minardi, *Phys. Rev. Lett.* **103**, 043201 (2009).
[18] S.-K. Tung, K. Jiménez-García, J. Johansen, C. V. Parker, and C. Chin, *Phys. Rev. Lett.* **113**, 240402 (2014).
[19] R. Pires, J. Ulanis, S. Häfner, M. Repp, A. Arias, E. D. Kuhnle, and M. Weidemüller, *Phys. Rev. Lett.* **112**, 250404 (2014).
[20] K. Helfrich, H.-W. Hammer, and D. S. Petrov, *Phys. Rev. A* **81**, 042715 (2010).
[21] N. T. Zinner and N. G. Nygaard, *Few-Body Syst.* **56**, 125 (2015).
[22] Y. Wang, J. Wang, J. P. D'Incao, and C. H. Greene, *Phys. Rev. Lett.* **109**, 243201 (2012).
[23] D. Blume and Y. Yan, *Phys. Rev. Lett.* **113**, 213201 (2014).
[24] B. Acharya, C. Ji, and L. Platter, *Phys. Rev. A* **94**, 032702 (2016).
[25] E. Braaten, H.-W. Hammer, D. Kang, and L. Platter, *Phys. Rev. A* **78**, 043605 (2008).
[26] D. S. Petrov and F. Werner, *Phys. Rev. A* **92**, 022704 (2015).
[27] G. V. Skorniakov and K. A. Ter-Martirosian, *Sov. Phys. JETP* **4**, 648 (1957).
[28] P. F. Bedaque, H.-W. Hammer, and U. van Kolck, *Nucl. Phys. A* **646**, 444 (1999).
[29] C. Ji, D. R. Phillips, and L. Platter, *Annals Phys.* **327**, 1803 (2012).
[30] K. Helfrich and H.-W. Hammer, *J. Phys. B* **44**, 215301 (2011).
[31] V. Efimov, *Nucl. Phys. A* **210**, 157 (1973).
[32] O. I. Kartavtsev and A. V. Malykh, *JETP Letters* **86**, 625 (2008).
[33] P. F. Bedaque, H.-W. Hammer, and U. van Kolck, *Phys. Rev. Lett.* **82**, 463 (1999).
[34] H.-W. Hammer and T. Mehen, *Nucl. Phys. A* **690**, 535 (2001).
[35] J. H. Hetherington and L. H. Schick, *Phys. Rev.* **137**, B935 (1965).
[36] E. Braaten, H. W. Hammer, and G. P. Lepage, *Phys. Rev. A* **95**, 012708 (2017).

- [37] E. Braaten, H. W. Hammer, and G. P. Lepage, *Phys. Rev. D* **94**, 056006 (2016).
- [38] B. D. Esry, C. H. Greene, and H. Suno, *Phys. Rev. A* **65**, 010705 (2001).
- [39] R. S. Bloom, M.-G. Hu, T. D. Cumby, and D. S. Jin, *Phys. Rev. Lett.* **111**, 105301 (2013).
- [40] J. Ulmanis, S. Häfner, R. Pires, F. Werner, D. S. Petrov, E. D. Kuhnle, and M. Weidemüller, *Phys. Rev. A* **93**, 022707 (2016).
- [41] J. P. D’Incao and B. D. Esry, *Phys. Rev. A* **73**, 030702 (2006).
- [42] J. J. Zirbel, K.-K. Ni, S. Ospelkaus, J. P. D’Incao, C. E. Wieman, J. Ye, and D. S. Jin, *Phys. Rev. Lett.* **100**, 143201 (2008).
- [43] L. J. Wacker, N. B. Jørgensen, D. Birkmose, N. Winter, M. Mikkelsen, J. Sherson, N. Zinner, and J. J. Arlt, *Phys. Rev. Lett.* **117**, 163201 (2016).
- [44] R. A. W. Maier, M. Eisele, E. Tiemann, and C. Zimmermann, *Phys. Rev. Lett.* **115**, 043201 (2015).
- [45] C. Ji, E. Braaten, D. R. Phillips, and L. Platter, *Phys. Rev. A* **92**, 030702 (2015).